Comparison of discharging electrodes for the electrostatic precipitator as an air filtration system in air handling units (Secondary Publication)†

Dong Ho Shin[1], Chang Gyu Woo[1], Hak-Joon Kim[1], Yong-Jin Kim[1], Bangwoo Han[1*]

[1] *Department of Environmental Machinery, Korea Institute of Machinery & Materials, Gajeongbuk-ro 156, Yuseong-gu, Daejeon, Korea.*

Abstract

The quality of indoor air is of increasing concern because it is closely related to human health. An air handling unit (AHU) can be used to control the quality of indoor air with respect to particulate matter and CO_2, as well as providing air conditioning by regulating the temperature and humidity of the air. Electrostatic precipitators have high collection efficiencies and low pressure drops. However, their chargers can generate ozone, which is a drawback of applying them to indoor air control. In this study, we compared four discharging electrodes: a 50-μm tungsten wire, a 100-μm tungsten wire, a 16-μm aluminum (Al) foil, and a carbon fabric comprised of 5–10-μm fibers. The carbon-fabric electrode exhibited superior particle collection efficiency and lower ozone generation for a given power consumption compared to the 50- and 100-μm tungsten wires, or the Al foil electrode. This low-ozone-generating, micro-sized electrode can be applied as an electrostatic precipitator in AHUs for indoor air control.

Keywords: Air handling unit; Carbon fabric; Discharge electrode; Ozone

[*] Corresponding author. Tel: 82-42-868-7608; Fax: 82-42-868-7284

E-mail address: bhan@kimm.re.kr

† This article is an English version of "Comparison of discharging electrodes for the electrostatic precipitator as an air filtration system in air handling units [Korean]" published in the Particle and Aerosol Research in March. 2017.

INTRODUCTION

The importance of indoor air quality and the level of public interest in the effects of fine particles on health are both increasing. Ozone is one of the substances found in indoor air that poses a threat to human health because it has adverse effects on the entire respiratory system. Ozone is relatively stable, and is generated mainly outdoors by sunlight. However, it can be generated inside by printers or photocopiers (Boelter and Davidson, 1997; Weschler, 2000).

Air handling units (AHUs) are typically used to improve the quality of indoor air via their filtering action. Electrostatic precipitators are used for industrial AHU filters. These have a relatively low pressure drop and are more efficient. However, they are not widely used because they can generate indoor ozone. Ozone filters can be used to collect the ozone generated by electrostatic precipitators, but these incur additional costs and require management. Carbon nanotubes (Bo et al., 2010) and graphene (Bo et al., 2011) have been used as discharge electrodes with lower ozone emissions, but there are difficulties associated with the use of such materials. Grob et al. (2013) developed a charging device based on ultraviolet (UV) light that generates very low amounts of ozone. However, UV generation consumes a large amount of energy. Hyun et al. (2017) reported a reduction in the amount of ozone generated by using coated discharge electrodes with silver, but the addition of this coating necessitates an additional step in the device fabrication process.

In this study, a new charging device consisting of a sheet of carbon fiber with a diameter of 5–10 μm was fabricated. Carbon-fiber electrodes can generate large numbers of ions at either the cathode or the anode while emitting minimal levels of secondary pollutants such as ozone (Han et al., 2009; Park et al., 2011). The particle-collecting performance and ozone emission of our charging device made of carbon fabric were compared to those of a conventional discharge electrode with 50- or 100-μm tungsten wire and aluminum (Al) foil. A collector at the rear end

was used to evaluate the collection performance of the carbon-fabric discharge electrode. This study can probably contribute to the improvement of indoor air quality with high efficiency by reducing the operating costs of AHUs with a low pressure drop, which is a key advantage of electrostatic precipitators (Kang et al., 2016; Han et al., 2012; Koo et al., 2013).

EXPERIMETAL SETUP AND METHODS

Fig. 1 shows optical images of the four discharge electrodes investigated in this study. Tungsten wires were prepared with diameters of 100 μm and 50 μm from 99.95% tungsten (AVENTION, Korea). The carbon-fabric electrodes were prepared M34-21 carbon sheet (1322P), which has 3K yarn with a plain weaving pattern of density 14 count $inch^{-1}$, purchased from Mirae Sinsojae (Korea). Aluminum foil with a thickness of 16 μm was purchased from Daehan Aluminum (Korea), and cut into 15 × 30-mm rectangles.

As shown in Fig. 2, the four prepared discharge electrodes were positioned at the center between two stainless-steel (SS) ground plates. A negative voltage of several kV was applied between the discharge electrode and the ground plates to provide unipolar charging. The outer case of the charging device was made of nonconductive polyvinyl chloride (PVC).

The collector comprised seven SS plates, as shown in Fig. 3. A high voltage was applied across three of these plates, while the others were grounded, which generated an electric field so that particles collected inside the collecting device. The spacing between the plates was 3.2 mm, and the collector was designed so that most of the singly charged particles of diameter 0.3 μm that passed through it at -5 kV could be collected.

Fig. 3 shows the duct system used to evaluate the performance of the chargers in this study. Potassium chloride (KCl) particles were generated by injecting 1% KCl solution into an atomizer (model 3076; TSI, USA) to produce test particles 0.3 μm in diameter and then supplied to the

77 upstream side of the 32 × 32-mm test duct. The particles then mixed with test air introduced by a
78 blower located downstream of the test duct.
79 The number concentration of 0.28~0.3-μm particles was maintained within 1×10^3 cm^{-3}
80 upstream of the duct. To minimize the inflow of contaminating particles, a high-efficiency
81 particulate air (HEPA) filter was installed upstream of the test duct. The charged particles
82 generated by the particle generator were neutralized with a ^{85}Kr neutralizer (model 3012; TSI).
83 The air flow rate was set to 12 L min^{-1} (face velocity, 0.3 m s^{-1}) for comparisons of the particle
84 collection efficiency. The 0.3-μm-particle collection performance and ozone concentration were
85 measured at different applied voltages, from -4 to -9 kV, and a fixed voltage of -5 kV was applied
86 to the collector. The particle number concentration and ozone concentration were measured using
87 a dust spectrometer (model 1.109; Grimm Aerosol Technik Ainring GmbH & Co. KG, Germany)
88 and ozone meter (Model 202; 2B Technologies, USA), respectively. Particle sampling was
89 conducted at a location downstream of the collector. The particle collection efficiency was
90 calculated using the equation:
91

$$\eta = \left(1 - \frac{n_1}{n_0}\right) \times 100$$

92
93 where
94 η = particle collection efficiency (%),
95 n_0 = number concentration of condition with charging device off and collector on (cm^{-3}), and
96 n_1 = number concentration of condition with charging device on and collector on (cm^{-3}).
97

98 **RESULTS AND DISCUSSION**
99

Fig. 4 shows the change in current according to the voltage applied over the charging device. The current was measured by connecting the discharge to the ammeter and the ground plate in series. Higher currents were measured at the same applied voltage in the order of a carbon fabric, 50-μm tungsten wire, 100-μm tungsten wire and Al foil. The currents increased when the size of the discharge electrode decreased in the cases of the carbon fabric, 50-μm tungsten wire, and 100-μm tungsten wire, but the discharge electrode of the Al foil was smaller than the discharge electrodes of the wire type used in this experiment, and this device had the highest onset voltage, of -8 kV. The thickness of the Al foil was 16 μm. However, the ductility of the Al foil electrode caused it to have a rough surface during the preparation steps.

Fig. 5 shows the collection efficiency with respect to the voltage applied over the discharge electrode. The discharge current increased with the applied voltage because higher discharge currents arise when more ions are generated at the discharge electrode. This increases both the probability of charging the particles and the collection efficiency of the collector. Fig.s 4 and 5 show that higher collection efficiency can be reached by using a discharging electrode with a higher discharging current at the same voltage. Comparing the two tungsten wire-discharge electrodes, which were made from the same material but had different diameters, the collection efficiency of the smaller tungsten wire electrode (diameter of 50 μm) was higher at the same applied voltage. The carbon-fabric discharge electrodes had markedly higher collection efficiencies than the 50-μm tungsten wire electrode because of their smaller diameter.

Fig. 6 shows the collection efficiency as a function of power consumption. The highest particle-collection efficiency at a given power consumption was obtained using the carbon-fabric discharge electrode. In the case of the tungsten wire, the 50-μm tungsten wire had higher particle collection efficiency than the 100-μm tungsten wire at the same power consumption. Although

the Al foil electrode was smaller than the wires, at the same voltage and power consumption its collection efficiency was lower because of its higher onset voltage.

Fig. 7 shows the changes in ozone concentration as a function of power consumption for each discharge electrode. Ozone measurement was performed 200 mm downstream of the charging device without using a collector with an airflow of 7 $L \cdot min^{-1}$. When the power consumption was held constant to within 0.5 W, the carbon-fabric discharge electrode generated several to several tens of ozone parts per billion, which was significantly fewer (10 times lower) than the other discharge electrodes, which generated several hundred ozone parts per billion. These results show that the carbon-fabric charging device developed was superior to the other charging devices tested in terms of both power consumption and ozone generation.

However, due its small diameter of several micron, the durability of the charging device and whether particles become attached to the carbon fabric after prolonged use need to be considered. Additionally, the effect of humidity on particle-collection performance should also be considered in future studies, prior to applying our results to AHU collecting equipment.

CONCLUSION

In this study, the collection performance and amounts of ozone generated were evaluated while varying the voltage applied according to the type of discharge electrode in the charging device. The conclusions are as follows:

(1) For the same applied voltage, the discharge current and collection efficiency of the 50-μm tungsten wire was higher than that of the 100-μm tungsten wire usually used in electrostatic AHU precipitators. Carbon fabric with a smaller discharge electrode was more effective than tungsten wire.

(2) At the same power consumption, the carbon-fabric discharge electrode generated less ozone than the other electrodes.

(3) Considering power consumption, particle collection performance, and ozone generation, the carbon-fabric discharge electrode was superior to the 50- and 100-μm tungsten wire discharge electrodes usually used in conventional electrostatic precipitators.

Based on our results, to improve indoor air quality while maintaining a low pressure drop, carbon-fabric discharge electrodes can be considered for use as the electrostatic precipitator in AHU air filtration systems instead of the conventional fiber filters that require periodic cleaning and replacement. The use of several micro-sized carbon-fabric discharge electrodes yields excellent particle collection performance with low power consumption and little ozone generation.

ACKNOWLEDGMENTS

This research was supported by the Eco-Innovation Project operated by the Ministry of the Environment, Korea.

REFERENCES

Bo, Z., Yu, K., Lu, G., Cui, S., Mao, S. and Chen, J. (2011). Vertically oriented graphene sheets grown on metallic wires for greener corona discharges: Lower power consumption and minimized ozone emission. *Energ. Environ. Sci.* 4: 2525–2528.

Bo, Z., Yu, K., Lu, G., Mao, S., Chen, J. and Fan, F.-G. (2010). Nanoscale discharge electrode for minimizing ozone emission from indoor corona devices. *Environ. Sci. Technol.* 44: 6337–6342.

171 Boelter, K.J. and Davidson, J.H. (1997). Ozone generation by indoor, electrostatic air cleaners.
172 *Aerosol Sci. Technol.* 27: 689–708.
173 Eifert, A., Baier, T. and Hardt, S. (2013). Small onset voltages in negative corona discharges
174 using the edges of gold and aluminum foils as nano-structured electrodes. *Appl. Phys.*
175 *Lett.* 103: 023114.
176 Grob, B., Burtscher, H. and Niessner, R. (2013). Charging of ultra-fine aerosol particles by an
177 ozone-free indirect uv photo-charger. *Aerosol Sci. Technol.* 47: 1325–1333.
178 Han, B., Hudda, N., Ning, Z., Kim, H.-J., Kim, Y.-J. and Sioutas, C. (2009). A novel bipolar
179 charger for submicron aerosol particles using carbon fiber ionizers. *J. Aerosol Sci.* 40:
180 285–294.
181 Han, B., Kim, H.J., Kim, Y.J., Jang, J.S. and Lee, S.H. (2012). Collection efficiency and air
182 cleaning capacity of two-stage electrostatic precipitator for its application to indoor air
183 cleaning. *J. Korean Soc. Indoor Environ.* 9(3): 285-298.
184 Hyun, O., Baek, M., Moon, J. and Ahn, Y. (2017). Performance evaluation of two-stage
185 electrostatic air filter with low-ozone emission corona charger. *Particul. Sci. Technol.* 35:
186 71–76.
187 Kang, J.H., Cho, J.P., Nam, Y.K. and Song, J.H. (2016). Effect of humidity and applied electrical
188 power in non-thermal plasma using corona discharge for the removal of hydrogen sulfide.
189 *J. Odor Indoor Environ.* 15(3): 243-250.
190 Koo, T.Y., Kim, Y.M., Hong, J.H. and Hwang, J.H. (2013). A study on collecting electrode
191 design for developing electrostatic precipitator (ESP) of urban railway underground
192 tunnels. *Part. Aerosol Res.* 9(2): 79-87.

193 Park, J.H., Yoon, K.Y. and Hwang, J. (2011). Removal of submicron particles using a carbon
194 fiber ionizer-assisted medium air filter in a heating, ventilation, and air-conditioning
195 (HVAC) system. *Build. Environ.* 46: 1699–1708.
196 Song, S.-K., Kim, Y.-K. and Kang, J.-E. (2009). Characteristics of ozone concentrations around
197 an urban valley based on the intensive air quality measurement during spring and summer
198 of 2006. *J. Korean Soc. Atmos. Environ.* 25: 289-303.
199 Vu, T.P., Kim, S.H., Lee, S.B. and Bae, G.-N. (2011). Secondary nanoparticle formation by a
200 reaction of ozone and volatile organic compounds emitted from a commercial
201 dishwashing liquid. *Part. Aerosol Res.* 7: 1-8.
202 Weschler, C.J. (2000). Ozone in indoor environments: Concentration and chemistry. *Indoor Air*
203 10: 269–288.
204

205 **Fig. Captions**

206

207 **Fig. 1.** Picture of the charging element used in this study. A: tungsten wire 100 μm in diameter, B:
208 tungsten wire 50 μm in diameter, C: carbon fabric (thickness 5–10 μm), D: aluminum foil
209 (thickness 16 μm).

210 **Fig. 2.** Schematic of the charger used in this study.

211 **Fig. 3.** Schematic of the experimental setup for the measurement of particle collection efficiency.

212 **Fig. 4.** Changes in current with respect to the voltage applied to the ionizers by changing the
213 charger materials.

214 **Fig. 5.** Collection efficiency as a function of the voltage applied to the ionizers for different
215 charger materials.

216 **Fig. 6.** Collection efficiency as a function of the power consumption by ionizers composed of
217 different charger materials.

218 **Fig. 7.** Ozone concentration as a function of power consumption for each discharge electrode.

219

220

221

222

223

224

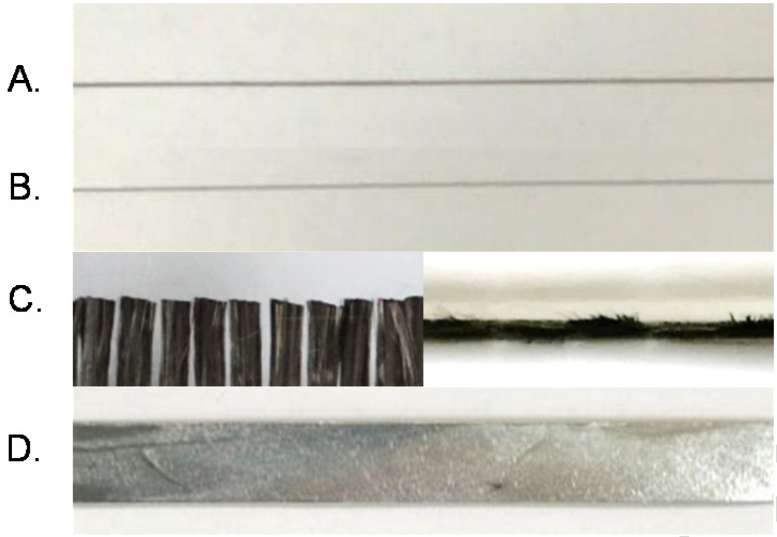

225

226

227 **Fig. 1.**

228

229

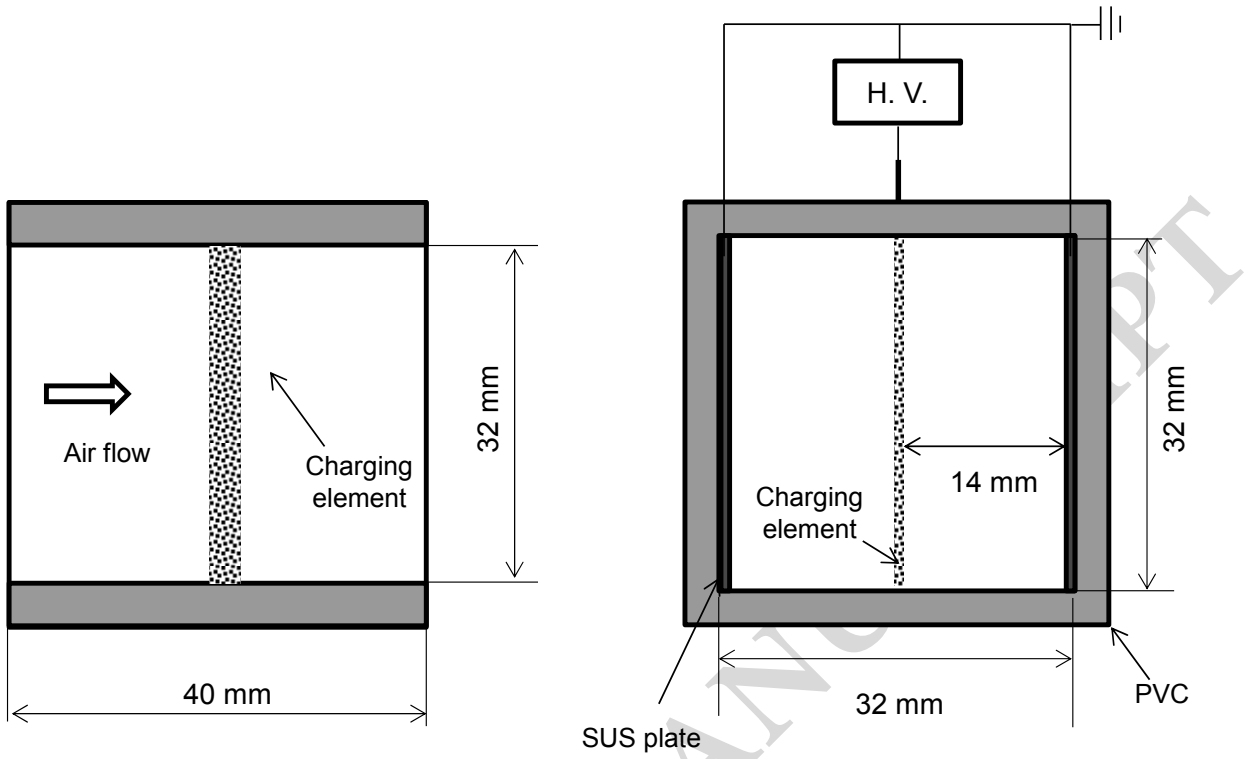

230

231

232 **Fig. 2.**

233

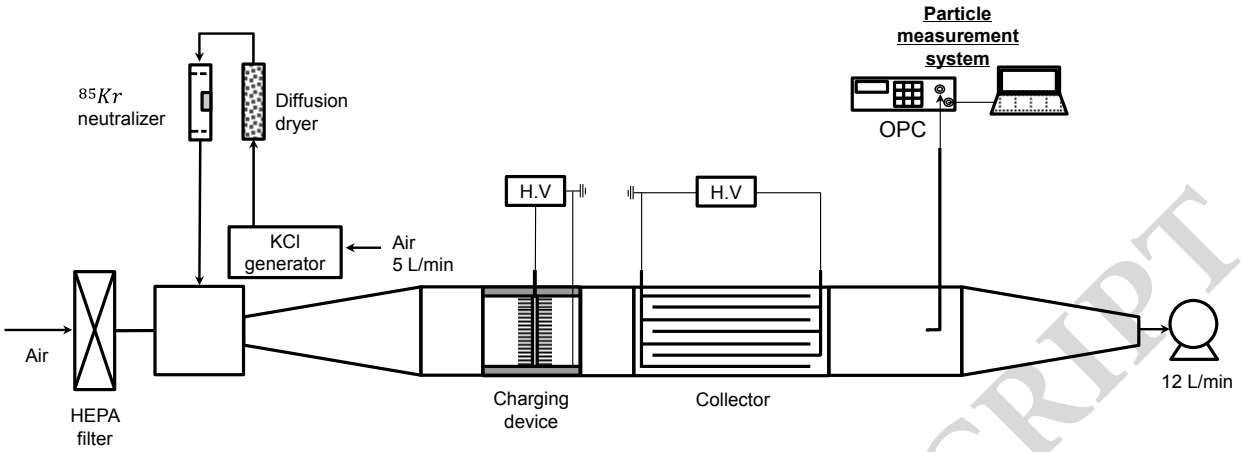

Fig. 3.

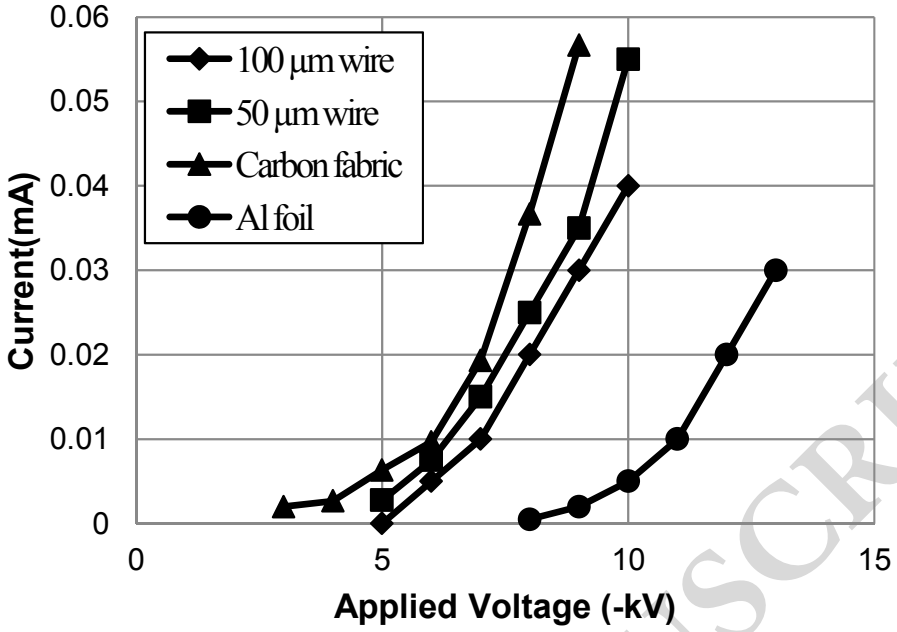

241

242

243

244

245 **Fig. 4.**

246

247

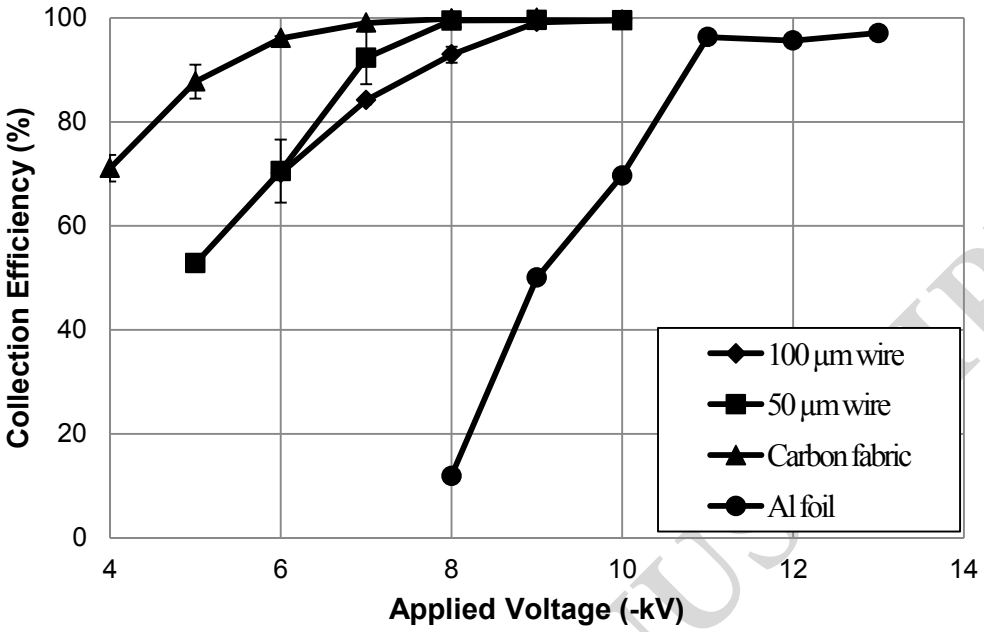

248

249

250 **Fig. 5.**

251

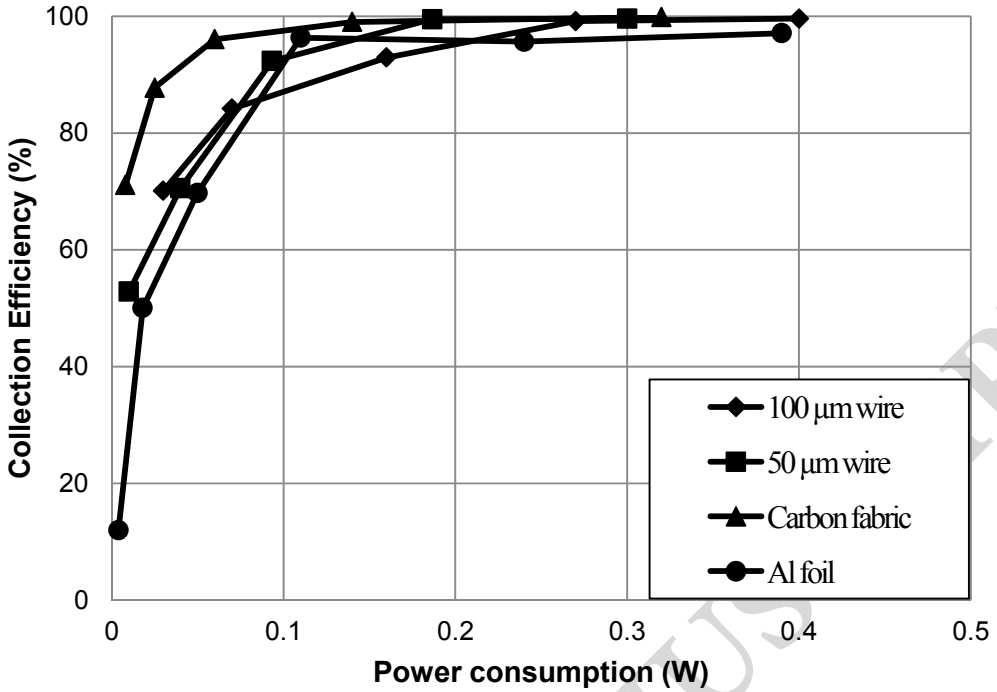

252

253 **Fig. 6.**

254

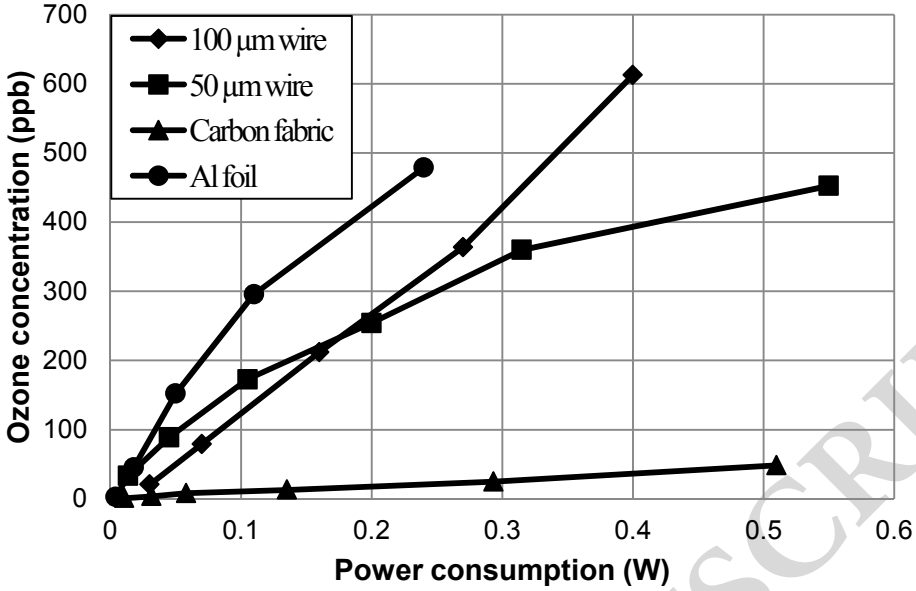

Fig. 7.

APPENDIX

The English in this document has been checked by at least two professional editors, both native speakers of English. For a certificate, please see:

http://www.textcheck.com/certificate/yXGt4V